IET Journals
The Institution of
Engineering and Technology

Identification of dominant low-frequency modes in ring-down oscillations using multiple Prony models

Darshana Prasad Wadduwage[1] ✉, Udaya D. Annakkage[1], Krish Narendra[2]

[1]Department of Electrical and Computer Engineering, University of Manitoba, Winnipeg, MB, R3T 5V6, Canada
[2]ERLPhase Power Technologies Ltd, Winnipeg, MB, R3Y 1G4, Canada
✉ E-mail: wdprasadmrt@gmail.com

Abstract: This study presents a simple approach to modify the Prony algorithm to extract dominant low-frequency modes present in ring-down oscillations in power systems. The proposed approach is based on the observation that true modes present in the ring-down oscillations appear consistently, irrespective of the order of the Prony model. It is shown that the consistently appearing modes can be extracted using a sorting method. The improved Prony algorithm which has the feature of extracting only the true modes present in the input signal is utilised to propose an oscillation monitoring algorithm in this study. The suitability of the proposed oscillation monitoring algorithm for real-time monitoring of low-frequency inter-area oscillations is demonstrated using synthetic signals and simulated signals of different test systems.

1 Introduction

Electromechanical oscillations are a characteristic of an interconnected electrical power system. Among different types of electromechanical oscillations, inter-area oscillations, which are the oscillatory modes involving the rotors of generators in different areas, have gained the attention of power system engineers. This is because a stable or a well-damped inter-area mode can become negatively-damped or poorly-damped due to changes in power system structure, operating conditions, and load characteristics [1]. As explained in [2, 3], one of the root causes for a major system collapse may be the unacceptable damping of an inter-area mode. Due to this reason, the power system may collapse due to gradually increasing rotor oscillations over several seconds. Therefore, continuous monitoring of poorly-damped modes provides the information on whether the power system is operating closer to the instability and is useful for initiating preventive control actions.

Real-time monitoring of power systems is facilitated by the availability of synchronised data from phasor measurement units (PMUs). PMUs provide time-tagged voltage and current phasors with respect to a common reference [4]. These data are available at the control centre at a higher rate compared to the traditional supervisory control and data acquisition system data, thereby facilitating a wide range of applications in power systems. However, these time series data need to be processed using appropriate algorithms to extract useful information for the operator.

The literature on monitoring small-signal rotor angle stability of the power system addresses two operating modes, (i) ambient or normal operation, and (ii) transient or ring-down operation [5]. Randomly changing load on the power system is the driving force behind the mode excitation in the ambient operation. In contrast, the transient operation relates to the non-linear behaviour of the power system subsequent to large-magnitude disturbances and the ring-down oscillations are observed in such situations. Thambirajah *et al.* [5] summarised different techniques used to assess the said stability under the two operating modes. The major area of interest in this study is the ring-down condition, which has been analysed using linear techniques, such as Prony [6], Kalman filter [7], Hankel total least squares [8], matrix pencil [9], Steiglitz-Mcbride and eigensystem realisation [10] algorithms. Furthermore, the algorithms based on the Hilbert–Huang transformation [11], and the Teager–Kaiser energy operator [12]

do not use linear approximations to determine the mode parameters in the ring-down oscillations. The multi-dimensional Fourier ring-down analysis algorithm applies the Fourier transform on multiple measurements in power systems to determine the mode parameters under the ring-down conditions [13] and the robust recursive least squares algorithm is capable of monitoring the low-frequency modes in both ambient and ring-down conditions [14].

In proposing these different algorithms, Prony algorithm has been treated as the reference for identifying the mode parameters in the ring-down oscillations in power systems. Commercially available software [15] has built-in Prony analysis tools, which are used for offline analysis. A major limitation of the Prony algorithm for real-time applications is the difficulty of extracting the dominant modes present in the signal among a large number of fictitious modes produced by the algorithm [6, 16]. As shown in [16] some of these fictitious modes may have poorer damping than the true modes, where the true modes represent the actual dynamic behaviour of the system. Therefore, it is important to separate the true modes from the fictitious modes. This issue has been addressed in the literature as explained below.

The energy of an oscillatory mode (E_i) can be calculated as, $E_i = \sum_{k=0}^{N-1} |x_i(k)|^2$ over a data window having N samples. Assuming that the dominant modes carry significant amounts of energies, they can be extracted if their energies are above a threshold value [16]. This threshold setting is difficult since, (i) the total energy of the input signal does not equal the sum of the energies of the individual modes, and (ii) when the input signal has a dc component; it subsequently carries a significant amount of energy. Another effort on extracting the true modes in the Prony analysis is to process multiple inputs simultaneously as proposed in [17]. This method is based on the assumption that an oscillatory mode can appear in different power system variables once the system is disturbed, hence the purpose is to determine a one set of mode estimates from multiple inputs. This method produces a large set of overdetermined equations to determine the mode parameters, which can still produce fictitious modes. The model reduction algorithm based on Akaike Information Criterion [18] and the minimal realisation method based on the singular value decomposition (SVD) algorithm [19] try to find the reduced-order model for the input signal. Eventually, the performance of each method is based on the closeness of the fit of the reduced-order model for the actual input signal. Zhou *et al.*

[16] used a stepwise regression which is an iterative procedure that adds and removes terms from the linear model based on their statistical significance in a regression to sort the dominant modes. The authors claim that this method works well under low signal-to-noise ratio (SNR) conditions. However, the damping ratio estimations of the Prony algorithm are sensitive to the presence of noise in the input signal.

The main contribution of this paper is to present a simple technique to extract the dominant modes from the Prony algorithm using a single input. The proposed algorithm is based on the observation that the dominant modes, which are characteristics of the power system, consistently appear in a measured response irrespective of the order of the Prony model. Such modes can then be extracted using a sorting method. Our simulation results show that the proposed algorithm is well suited for real-time monitoring of the small-signal rotor angle stability.

The rest of this paper is organised as follows. Theoretical background of the Prony algorithm and the rationale behind the modified algorithm are given in Section 2. Section 3 presents the proposed oscillation monitoring algorithm. The sensitivities of the proposed algorithm for different parameters are presented in Section 4. Section 5 evaluates the performance of the proposed algorithm. Finally, Section 6 presents the conclusions of the study.

2 Mathematical preliminaries

A brief review of the theory of Prony analysis is presented in Section 2.1 and the proposed algorithm is explained in Section 2.2.

2.1 Theory of Prony analysis

Prony analysis represents an input time-domain signal, $Y(t)$ in the form of $Y(t) = \sum_{i=1}^{p} A_i e^{\sigma_i t} \cos(2\pi f_i t + \varphi_i)$, where p is the order of the Prony model, f_i and σ_i are the frequency and the real part of the eigenvalue associated with the ith mode, respectively. A_i and φ_i are the amplitude and the phase angle of the ith mode, respectively. Theoretical derivations of this analysis are well documented in the literature [6, 16, 17]. In summary, the analysis involves the following steps:

(i) Construct a discrete linear prediction (LP) model that best fits the recorded signal.
(ii) Find the roots of the characteristic polynomial associated with the LP model and thereby the eigenvalues.
(iii) Determine the least-squares solution of the original set of equations in order to determine the amplitude and the phase angle of each mode.
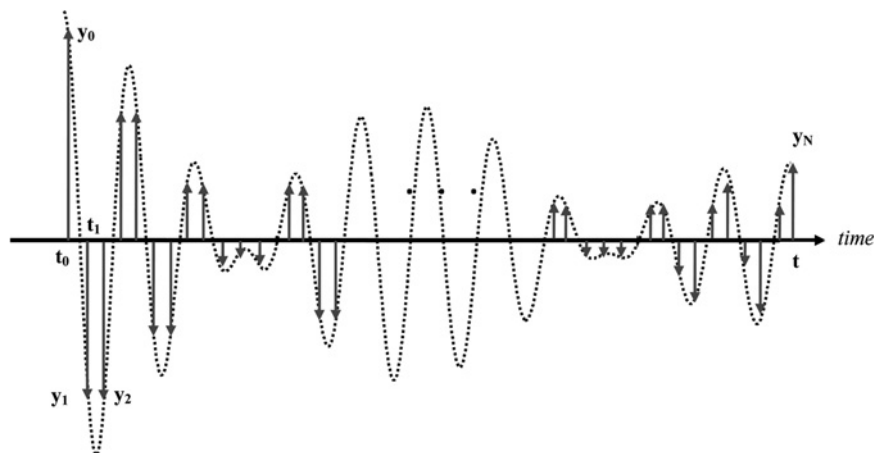
The performance of the Prony algorithm depends on the solution for p number of unknowns using $(N - p)$ number of equations in step (ii) above, where N is the total number of samples over the data window. In order to suppress the effect of noise, it is the usual practice to over fit the input signal. For example, the order p of the Prony model is selected as $p \leq (N/3)$ [16]. Therefore, fictitious modes are introduced into the calculation in addition to the true modes present in the input signal. It is important to extract the true modes from the fictitious modes for real-time applications.

2.2 Rationale behind the proposed algorithm

The waveform shown in Fig. 1 is a synthetically generated signal at a known sampling rate. This signal consists of two oscillatory modes at frequencies 0.5, 0.6 Hz and damping ratios 1.5, 1.6%. Consider two data sets of the waveform; $Y_1 = [y_0, y_1, y_2, \ldots, y_N]_{1 \times N}$ and $Y_2 = [y_0, y_2, y_4, \ldots, y_N]_{1 \times (1+(N/2))}$, where y_k is the value at the kth sampling time. Note that the lengths of the two data sets are different. Such different length data sets can be selected using two approaches, (i) changes the data window length keeping the sampling time fixed, and (ii) down-sample the data keeping the data window length fixed. Coefficients of the two LP models given in (1) and (2) can be determined using the Prony analysis as explained in Section 2.1 on these two data sets. Note that the orders of the two LP models p_1 and p_2 are different since the sizes of the two data sets are different

$$Y_1 \rightarrow y_1(k)$$
$$= a_1 y_1(k-1) + a_2 y_1(k-2) + \cdots + a_{p_1} y_1(k - p_1) \quad (1)$$

$$Y_2 \rightarrow y_2(k)$$
$$= b_1 y_2(k-1) + b_2 y_2(k-2) + \cdots + b_{p_2} y_2(k - p_2) \quad (2)$$

These two LP models have the characteristic equations given in (3) and (4), where the roots of the characteristic equations are the discrete domain poles of the linear system

$$(1) \rightarrow z^{p_1} - a_1 z^{p_1 - 1} - a_2 z^{p_1 - 2} - \cdots - a_{p_1 - 1} z - a_{p_1}$$
$$= (z - z_{11})(z - z_{12}) \cdots (z - z_{1p_1}) \quad (3)$$

$$(2) \rightarrow z^{p_2} - b_1 z^{p_2 - 1} - b_2 z^{p_2 - 2} - \cdots - b_{p_2 - 1} z - b_{p_2}$$
$$= (z - z_{21})(z - z_{22}) \cdots (z - z_{2p_2}) \quad (4)$$

The number of roots in (3) and (4) are p_1 and p_2, respectively, where $p_1 \neq p_2$. However, these two characteristic equations represent an
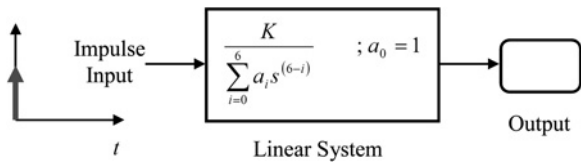

Fig. 1 *Digitised synthetic signal*

Fig. 2 *Test linear system*

Table 1 Test signal I parameters

Mode no	Frequency, Hz	Real part of the eigenvalue	Damping ratio, %
1	0.5	−0.0471	1.5
2	0.6	−0.0603	1.6
3	0.7	−0.5541	12.5

Table 2 Modes appearing in different length data windows

Window 1: 0–7 s		Window 2: 0–8 s	
Frequency, Hz	Real part of eigenvalue	Frequency, Hz	Real part of eigenvalue
0.5	**−0.0471**	**0.5**	**−0.0471**
0.6	**−0.0603**	**0.6**	**−0.0603**
0.7	**−0.5541**	**0.7**	**−0.5541**
1.4777	−0.5420	1.3763	−0.7802
1.9417	−0.6705	1.7855	−0.9865
2.3874	−0.7636	2.1781	−1.1396
2.8260	−0.8378	2.5643	−1.2634
3.2612	−0.8999	2.9471	−1.3681
3.6942	−0.9534	3.3280	−1.4589
4.1259	−1.0004	3.7077	−1.5393
4.5567	−1.0424	4.0864	−1.6114
4.9868	−1.0804	4.4645	−1.6767
		4.8421	−1.7365

identical linear system having two oscillatory modes with the parameters mentioned at the beginning of this section. Each oscillatory mode is related with a pair of complex conjugate roots in the characteristic equation. Therefore, theoretically there should be four common roots in this case among p_1 and p_2. These roots describe the true dynamic behaviour of the linear system and the remaining roots [$(p_1 - 4)$ in (3) and $(p_2 - 4)$ in (4)] are the fictitious roots produced by the linear fitting.

In order to illustrate the said theoretical explanation, consider the system shown in Fig. 2, having three oscillatory modes with the parameters mentioned in Table 1. This system was simulated in MATLAB/SIMULINK using 60 samples/s sampling rate, which adheres to the IEEE standard for synchrophasor measurements in power systems [4]. Prony analysis was individually applied on the output of this system using two data windows in lengths 7 and 8 s, respectively. Table 2 shows the frequencies and the real parts of the eigenvalues determined in these two cases. Only the modes with frequencies less than 5 Hz are shown.

Table 2 shows that the consistently appearing modes (shown in bold) in the two windows are the true modes of the input signal. By selecting data windows of different lengths, the order of the LP model used in the Prony algorithm is changed which impacts on the fictitious modes, but not on the true modes of the input signal as illustrated in Table 2.

The order of the linear fitting in the Prony analysis can also be changed by changing the sampling time keeping the data window length fixed. This approach is applicable when the PMU data are available at a higher reporting rate. Annex C of [4] describes how multiple rate outputs can be generated from the same PMU. An 8 s long data window of the above signal was analysed using 10, 15, and 30 samples/s sampling rates. This analysis also showed that the true modes of the input signal to appear consistently.

The core of the Prony analysis is a linear approximation to the input signal as explained in this section. The rationale behind the improved Prony algorithm is the observation that the true modes present in the input signal appear consistently when the order of the Prony models is varied. However, it is an inherent characteristic of the power system to have additional modes introduced by the non-linear mode interactions due to its dynamic behaviour. These effects have been investigated in several publications on normal form analysis [20, 21]. For example, if λ_k and λ_l are two individual modes present in the linear system, the same system exhibits combination modes $(\lambda_k + \lambda_l)$ when it is subjected to a large disturbance. It is illustrated in [21] that these combination modes, $e^{(\lambda_k+\lambda_l)t}$ are more heavily damped than the first-order modes, $e^{\lambda_k t}$ or $e^{\lambda_l t}$. As a result, they do not appear in multiple windows. Another point to note is that the highly-damped first-order modes may also not appear in multiple windows. The goal of the proposed algorithm is to identify the poorly-damped low-frequency modes. The properties discussed above are helpful in achieving this goal.

2.3 Extracting true modes of the input signal

In this study, the Euclidean distances between individual modes in the complex plane were compared to extract the consistently appearing modes. Assume that p_1 and p_2 are the number of modes identified by the Prony analysis using two data windows or sampling steps as explained in Section 2.2. Thus, the true modes can be extracted using the following logic:

$$
\begin{aligned}
&\text{if, } \sqrt{\left(f_i - f_j\right)^2 + \left(\sigma_i - \sigma_j\right)^2} \leq \tau \quad i = 1, 2, \ldots, p_1 \\
&\quad j = 1, 2, \ldots, p_2 \\
&\quad f = \frac{f_i + f_j}{2} \\
&\quad \sigma = \frac{\sigma_i + \sigma_j}{2}
\end{aligned}
\tag{5}
$$

where τ is the threshold assigned to identify the close modes, and f and σ refer to the frequency and the real part of the eigenvalue of the true mode.

2.4 Improved Prony algorithm

The procedure of the improved Prony algorithm is summarised below:

(i) Specify the main data window length and the sampling time step.
(ii) Change the order of the LP model used in the Prony analysis. Two possible options for changing the order are as follows:
 • Reduce the length of the data window in intervals of 1 s keeping the specified sampling time fixed. Multiple sub-windows can be generated inside the main data window via this approach. This is called the **shrinking window improved Prony algorithm**.
 • Change the sampling time keeping the data window length fixed. This is called the **multiple sampling time improved Prony algorithm**.
(iii) Apply the Prony analysis individually on each case. Extract only the eigenvalues with positive frequencies less than 5 Hz.
(iv) Extract the true modes and determine their parameters as explained in Section 2.3.

The complex eigenvalues always occur in conjugate pairs, where each pair corresponds to a single oscillatory mode. Further, we are interested in the low-frequency oscillatory modes. Hence, the number of combinations to be checked to extract the true modes can be reduced by selecting only the positive-frequency eigenvalues with frequency less than 5 Hz. The improved Prony algorithm that employs multiple sampling times can be applied

only when the PMU data are available at a higher reporting rate. However, a PMU reporting rate of 10 samples/s is sufficient to observe the inter-area modes. Thus the analyses presented in this paper are based on the shrinking window improved Prony algorithm.

2.4 Implementation

The length of the main data window of the algorithm was selected as four cycles of the dominant inter-area mode, as recommended in [22]. In the cases where there is no idea about this frequency, it is recommended to set the length of the first data window to be 10–20 s assuming the lowest frequency as 0.2 Hz. The lengths of all the subsequent data windows can be selected using the actual frequency of the dominant mode determined by the algorithm. The data are available at the recommended PMU reporting rates for the application. These are 10, 12, 15, 20, 30, 60, 100, and 120 samples/s [4]. The sensitivities of the proposed algorithm to the change in the data window length and the sampling rates are analysed in Section 4.

The shrinking window algorithm is implemented as a block processing algorithm as shown in Fig. 3. The order p of the Prony model was selected as $(N/3)$ as explained in Section 2.1. The least-squares solution for the coefficients of the LP model was determined using truncated SVD [19]. The truncation parameter can be identified when the energy ratio (ER) value defined in (6) is sufficiently close to unity

$$\mathrm{ER}(q) = \frac{\sum_{i=1}^{q} \alpha_i^2}{\sum_{i=1}^{p} \alpha_i^2} \qquad (6)$$

where α_i is the ith singular value of the data matrix.

3 Proposed oscillation monitoring algorithm

The oscillation monitoring algorithm proposed in this paper is shown in Fig. 4 and was implemented in MATLAB in the PC environment.
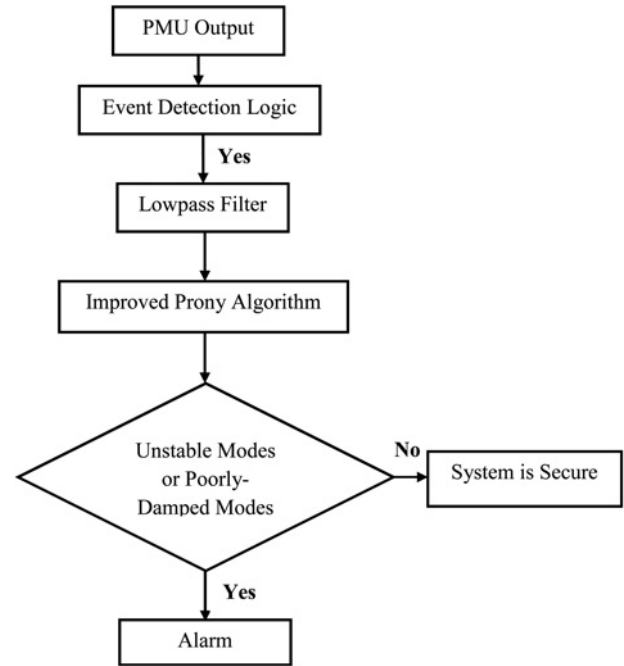

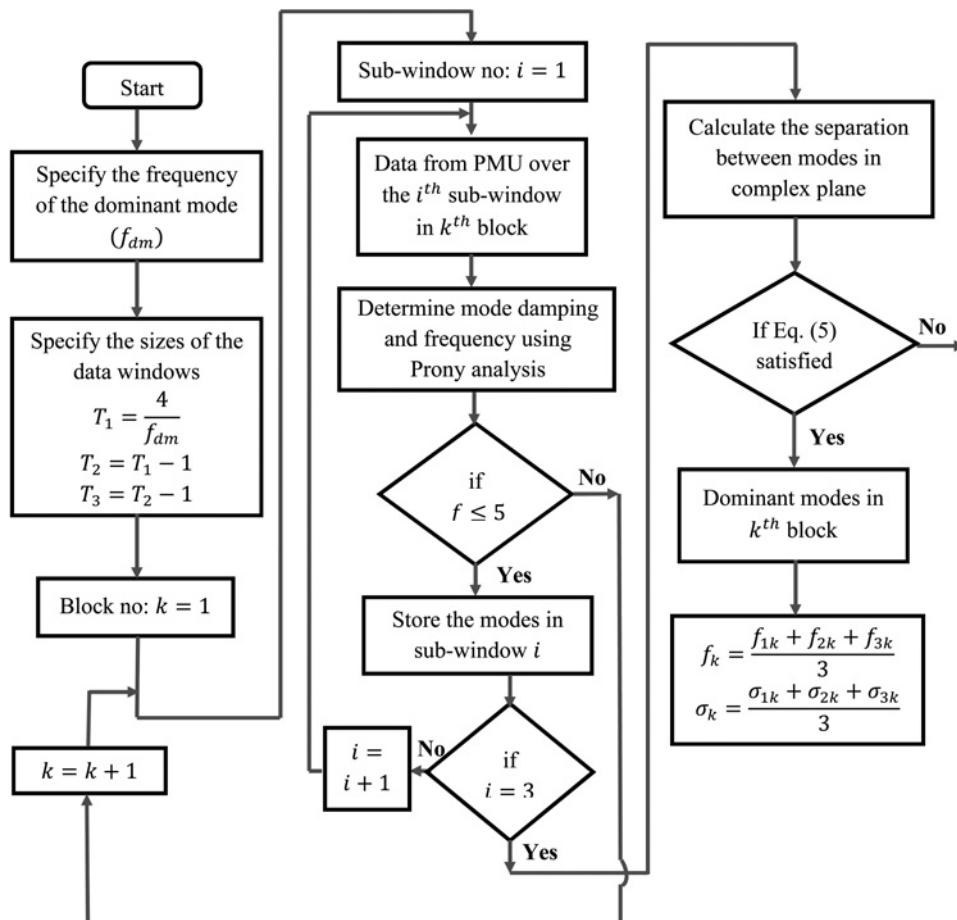**Fig. 4** *Proposed oscillation monitoring algorithm*

Fig. 3 *Flowchart of the shrinking window improved Prony algorithm*

The Prony algorithm works when there is a noticeable oscillation in the data window [6]. Thus, it is important to apply the algorithm into right data type. Subsequent to an onset of a ring-down oscillation in the system, the energy of the measured signal in the data window, $E_k = \sum_{i=k}^{k+N-1} |x(i)|^2$ dramatically changes compared to the mean energy in the ambient operation [23]. This feature can be used to detect the onset of a ring-down oscillation and hence to initiate the improved Prony algorithm. In this study, the improved Prony algorithm is initiated, if E_k is continuously changing and if $E_k \geq 1.05 \times \text{mean}(E_1 : E_{k-1})$ or $E_k \leq 0.95 \times \text{mean}(E_1 : E_{k-1})$.

After identifying a ring-down condition, the measured signal is sent through a low-pass filter which, (i) separates the low-frequency oscillatory modes in the measured signal, (ii) reduces the influence of the measurement noise on the mode estimation, and (iii) enhances the true mode extraction capability of the improved Prony algorithm under low SNR conditions. In this study, the specifications used to design the filter were, (i) 2 Hz pass-band corner frequency, (ii) 5 Hz stop-band corner frequency, (iii) 0.2 dB ripple in the pass-band, and (iv) 20 dB ripple in the stop-band. The attenuation levels used are same as those recommended in [4] to improve the dynamic performance of the PMU. A finite impulse response (FIR) filter was designed for this application to meet the above specifications using the Hamming window [24]. The FIR filters are considered to be efficient filters due to their linear phase characteristics and are always stable [24]. The filter output signal is then processed by the improved Prony algorithm as explained in Section 2.

The improved Prony algorithm determines whether the oscillations present in the power system have adequate damping or not. If the oscillatory modes are poorly-damped, the operator is alerted to initiate the necessary control actions. If not the ring-down oscillations will decay since all the oscillations have adequate damping and the power system enters into an ambient condition again. After concluding the oscillatory stability status, the algorithm is reset to check for the occurrence of a ring-down condition in the power system again. Therefore, the proposed algorithm is continuously executing in the real-time environment.

4 Sensitivity analyses

This section presents the sensitivities of the shrinking window improved Prony algorithm on different parameters using the synthetic signal given in (7). The frequencies and the damping ratios of the oscillations present in the signal are 0.25, 0.39 Hz and 7, 6.5%, respectively. This signal has been used in [16] to illustrate the true mode extraction capability of the Prony algorithm under noisy conditions using a stepwise regression analysis.

$$x(t) = 2e^{-0.1102t} \cos(1.5708t + 1.5\pi) \\ + 2e^{-0.1596t} \cos(2.4504t + 0.5\pi) + \epsilon(t) \tag{7}$$

Assume a time step of (1/120) s and 30 dB SNR. It is the usual practice in power system literature to use a Monte Carlo method to evaluate the performance of the mode identification algorithms [14, 16]. The Monte Carlo method uses independent trials to generate different instances of the random noise, $\varepsilon(t)$. In this study, 100 independent simulations were done in this regard. Three measures were used to analyse the performance of the algorithm. These three measures were (i) a number of trials in which only the true modes were extracted (γ_1), (ii) the number of trials in which only one of the true modes was extracted (γ_2), and (iii) a number of trails in which the true modes and the fictitious modes were extracted (γ_3). If, $\gamma_1 + \gamma_2 + \gamma_3 < 100$, none of the modes were extracted in some trials.

In this case, the length of the data window for the Prony analysis was specified in terms of the number of cycles of the 0.25 Hz mode. The threshold used to extract the consistently appearing modes was changed in steps of 0.01. It was found that a data window of length 3 or 4 cycles of the dominant low-frequency mode with two sub-windows provide an acceptable mode extraction accuracy when the threshold value lies between 0.01 and 0.03.

4.1 Sensitivity analysis with change in measurement noise

To investigate the impact of the measurement noise on the mode parameter estimations by the Prony algorithm, the input signal was corrupted with measurement noise such that the SNR was 5, 10, 15, and 20 dB, respectively. A 16(=4/0.25) s long data window with two sub-windows were used to extract the dominant modes. Fig. 5 shows one instance of the synthetic signal at each SNR and the low-pass filter output. Tables 3 and 4 show the true mode extraction capability and the statistical significance of the estimated mode parameters with respect to the true mode parameters considering the 100 independent simulations.

The performance index γ_1 represents the probability of extracting only the true modes present in the input signal. As shown in Table 3, this probability is above 90% when the threshold value is 0.01–0.03
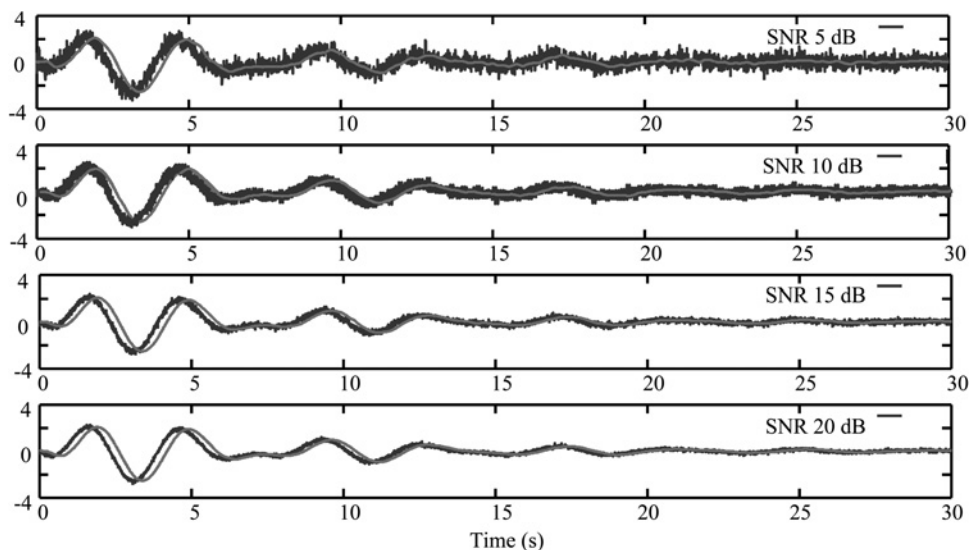

Fig. 5 *Synthetic signal and the low-pass filter output signal at different SNR levels, blue curve indicates input signal, red curve indicates low-pass filter output signal*

Table 3 Sensitivity analysis of the shrinking window algorithm with measurement noise

Noise level, dB	Threshold	γ_1	γ_2	γ_3
5	0.01	89	8	0
	0.02	98	0	2
	0.03	91	0	9
	0.04	82	0	18
	0.05	70	0	30
10	0.01	99	1	0
	0.02	95	0	5
	0.03	90	0	10
	0.04	81	0	19
	0.05	76	0	24
15	0.01	100	0	0
	0.02	97	0	3
	0.03	91	0	9
	0.04	86	0	14
	0.05	79	0	21
20	0.01	100	0	0
	0.02	98	0	2
	0.03	93	0	7
	0.04	89	0	11
	0.05	79	0	21

under different SNR conditions. Furthermore, the sensitivity analysis given in Section 4.3 with different sampling rates also illustrates that this probability is above 90% when the threshold value is 0.02. The interest in this study is to identify the low-frequency inter-area oscillations (0.1–1 Hz) and this threshold is a value assigned for the amount of deviation from the parameters of the true mode. Therefore, based on the sensitivity analyses, it is recommended to set the threshold value as 0.02 to sort the true low-frequency modes. The validity of this threshold value is further demonstrated in Section 5 using simulated cases of different test systems.

As shown in Table 4, the presence of measurement noise in the input signal has not degraded the performance of the algorithm. The deviations of the mode parameters even under noisy conditions are less. This is because the input signal is first sent through a low-pass filter. Thus, the filter output signal is less noise contaminated as observed in Fig. 5.

Table 4 Statistical significance of the shrinking window algorithm with measurement noise

Noise level, dB	Mode no.	Frequency, Hz	std	Real part of eigenvalue	std
5	1	0.2475	0.0006	−0.1107	0.0043
	2	0.3861	0.0011	−0.1595	0.0061
10	1	0.2500	0.0005	−0.1100	0.0030
	2	0.3899	0.0009	−0.1597	0.0045
15	1	0.2500	0.0003	−0.1100	0.0015
	2	0.3899	0.0005	−0.1598	0.0024
20	1	0.2500	0.0002	−0.1103	0.0009
	2	0.3900	0.0002	−0.1596	0.0015

4.2 Sensitivity analysis with change in sampling rate

IEEE standard for synchrophasor measurements in power systems [4] recommends 10, 12, 15, 20, 30, 60, 100, and 120 frames/s (fps) sampling rates for a 60 Hz system. The input signal given in (7) at 20 dB SNR was analysed using the oscillation monitoring algorithm to investigate the effect of the PMU reporting rates on the mode parameter estimation. A 16 s long data window with two sub-windows was used and the threshold value used to extract the dominant modes was 0.02. Table 5 summarises the results of the analysis.

It can be seen that the standard deviations of the mode parameters are very small ($< 10^{-2}$) indicating that their variations with the PMU reporting rates are negligible for the purpose of real-time oscillation monitoring. Thus, an adaptive sampling scheme as the one proposed in [25] is not necessary to the Prony analysis to monitor the low-frequency oscillations in real-time using synchronised data.

5 Results and discussion

This section evaluates the performance of the proposed oscillation monitoring algorithm using two test systems. Following specifications were used in the improved Prony algorithm; (a) 10 samples/s sampling rate, (b) two sub-windows inside the main data window, (c) 0.02 threshold value, and (d) 100 independent simulations. The standard deviations of the mode parameters in each case were calculated with respect to the true mode parameters determined by the eigenvalue analysis. Furthermore, the dc component of the input signal was removed prior to applying the improved Prony algorithm.

5.1 16-Generator 68-bus test system

The 16-generator 68-bus test system shown in Fig. 6 is a reduced order equivalent of the interconnected New England test system (NETS) and the New York power system (NYPS) [26]. This system was simulated using the detailed generator model. Further, all the generators were equipped with exciters and the generators 9, 13, and 16 were equipped with power system stabilisers. The four inter-area modes identified using the small-signal stability analysis are given in Table 6. The inter-area modes with frequencies 0.52 and 0.70 Hz are the two poorly-damped modes.

Dynamic simulation of the system for a contingency of clearing a solid three-phase bus fault at bus 18 after five cycles of the fundamental frequency (60 Hz) was done using a transient stability analysis tool (TSAT) [15]. The observability calculations reveal that both of the poorly-damped modes are observable in the active power flows along the tie lines connecting NETS and NYPS. Fig. 7 shows the active power flow along one of the tie lines connecting the buses 60 and 61. The fault was applied at time; $t = 5$ s.

The measurement noise at 30 dB SNR was added to the simulated signal and the data window length was set as four cycles of the 0.52
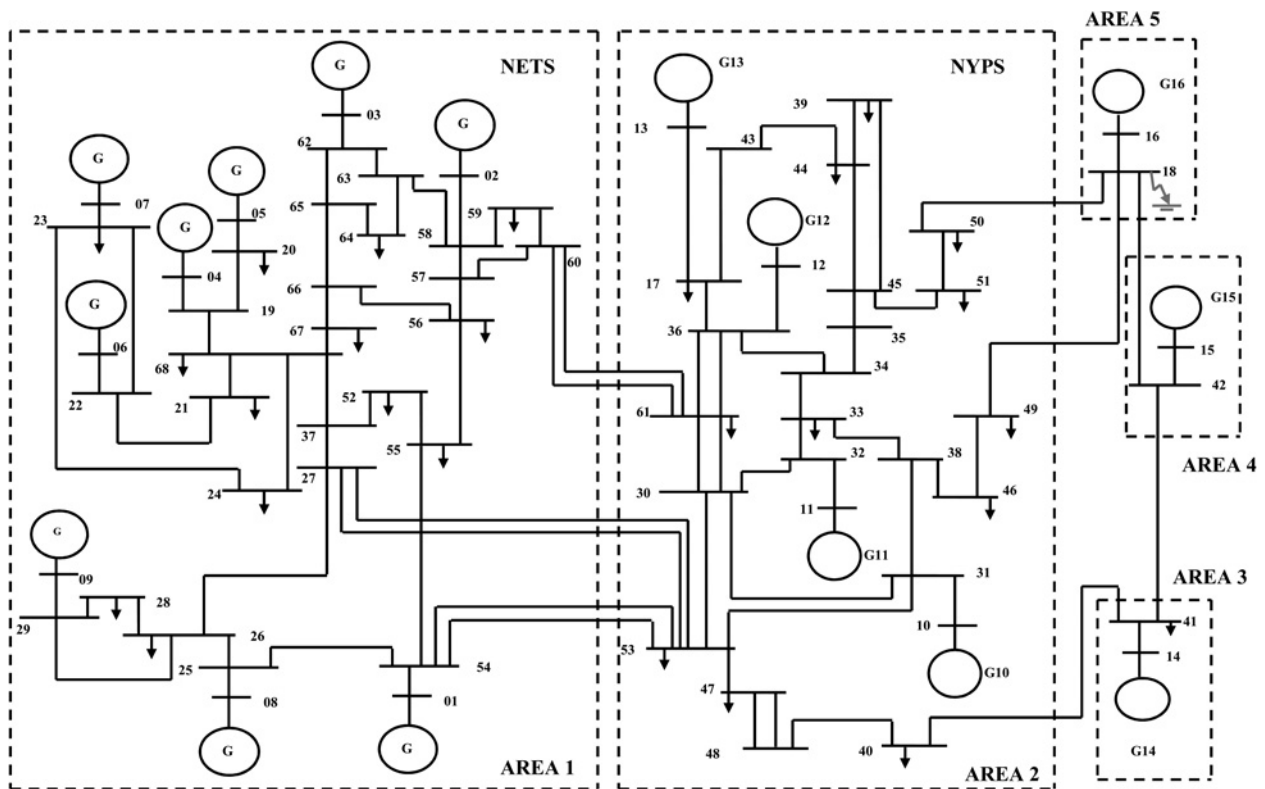
Table 5 Performance of the shrinking window algorithm with change in PMU reporting rate

Reporting rate, fps	γ_1	γ_2	γ_3	Mode no	Frequency, Hz	std	Real part of eigenvalue	std
10	94	0	6	1	0.2498	0.0007	−0.1107	0.0049
				2	0.3900	0.0011	−0.1611	0.0073
12	92	1	7	1	0.2500	0.0006	−0.1102	0.0039
				2	0.3901	0.0010	−0.1611	0.0065
15	96	0	4	1	0.2500	0.0005	−0.1107	0.0037
				2	0.3901	0.0008	−0.1598	0.0055
20	96	0	4	1	0.2501	0.0004	−0.1106	0.0026
				2	0.3899	0.0007	−0.1591	0.0043
30	92	0	8	1	0.2500	0.0003	−0.1100	0.0022
				2	0.3900	0.0005	−0.1599	0.0036
60	95	0	5	1	0.2500	0.0002	−0.1106	0.0015
				2	0.3900	0.0003	−0.1596	0.0018
100	95	0	5	1	0.2500	0.0002	−0.1102	0.0010
				2	0.3899	0.0003	−0.1594	0.0016

Fig. 6 *16-Generator 68-bus test system*

Table 6 Inter-area modes of the 16-generator 68-bus test system

Frequency, Hz	Real part of eigenvalue	Damping ratio, %	Inter-area mode
0.41	−0.3349	12.89	group of generators in NETS and NYPS against generators in area 4
0.52	−0.0480	1.47	generator 14 against generator 16
0.70	−0.0673	1.53	group of generators in NETS against generator 16
0.79	−0.2206	4.44	generator 15 against generator 14

Hz mode. The event detection logic identified an onset of a ring-down oscillation at time $t = 5.59$ s. Consider the two data windows, 6.0–14.0 s and 20.6–28.6 s selected soon after and few seconds later the contingency. The true mode extraction capabilities over the two windows were, $\gamma_1 = 81$, $\gamma_2 = 19$, $\gamma_3 = 0$ and $\gamma_1 = 97$, $\gamma_2 = 0$, $\gamma_3 = 3$, respectively, where γ_1, γ_2, and γ_3 are the same as those defined in Section 4. Table 7 shows the statistical significance of the mode parameters.

As shown in Table 7, the damping estimations may significantly deviate when a data window soon after the contingency is used. There are two possible reasons for this, (a) non-linearity of the power system response soon after the application of the disturbance [6], and (b) inability of the Prony algorithm to
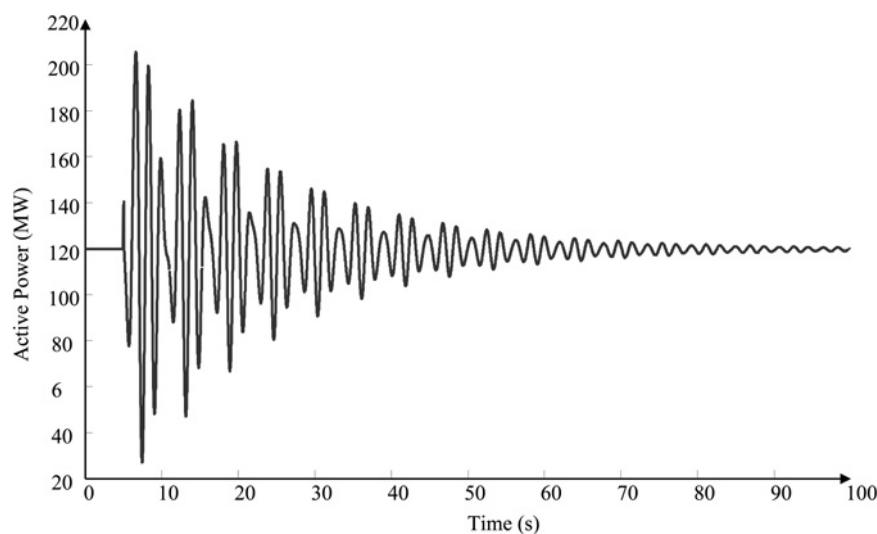

Fig. 7 *Active power flow along lines 60–61 subsequent to a contingency*

Table 7 Mode parameter estimations: 16-generator 68-bus test system

Mode no.	Parameter	Data window: 6.0–14.0 s		Data window: 20.6–28.6 s	
		Mean value	std	Mean value	std
1	fre., Hz	0.5205	0.0034	0.5216	0.0008
	real part of eigenvalue	−0.0101	0.0122	−0.0482	0.0008
2	fre., Hz	0.6989	0.0031	0.6994	0.0004
	real part of eigenvalue	−0.0743	0.0673	−0.0699	0.0034

Table 8 Mode parameter estimations: 50-generator 470-bus test system

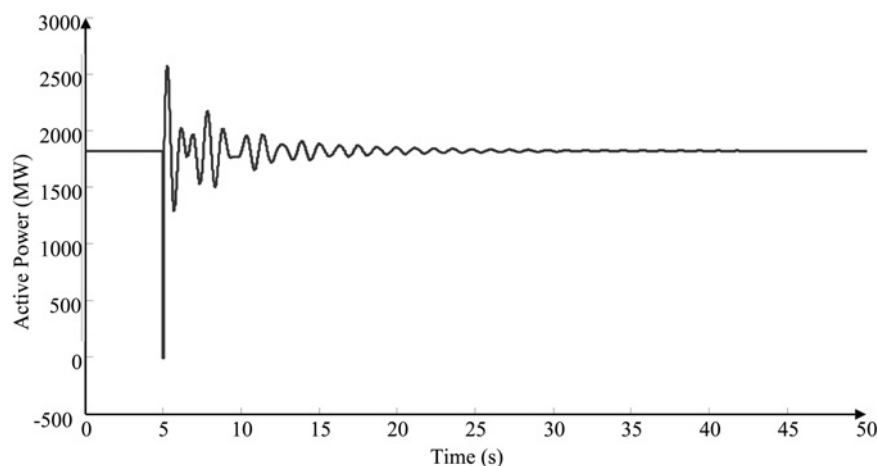| Mode no	Parameter	Data window: 5.92–15.92 s		Data window: 20.6–30.6 s	
		Mean value	std	Mean value	std
1	frequency, Hz	0.8223	0.0005	0.8223	0.0005
	real part of eigenvalue	−0.1528	0.0210	−0.1401	0.0082

accurately determine the mode damping when a poorly-damped mode is superimposed with a highly-damped mode. It was shown in Section 2.2 that the Prony algorithm correctly identifies the mode parameters even under the situations where the input signal consists of both highly-damped and lightly-damped modes. Therefore, the reason 'b' above can be eliminated. Thus, it is recommended to discard the initial damping estimations of the algorithm before initiating any preventive control actions.

5.2 50-Generator 470-bus test system

The 50-generator 470-bus [27] test system has two areas with 14 thermal generators in area 1 and 23 thermal generators and 13 hydro generators in area 2. The system was modelled using detailed generator models and exciters. The small-signal stability analysis identified a poorly-damped inter-area mode at 0.823 Hz frequency and 2.55% damping ratio between the two areas. The speed of the generator 16 highly participates in this inter-area mode. Dynamic simulation of the system was done using TSAT software subsequent to a contingency of clearing a solid three-phase bus fault applied at bus 16 after five cycles of the fundamental frequency without any topology change in the network. The fault was applied at time; $t = 5$ s. Fig. 8 shows the active power injected by the generator 16 into the network.

The simulated signal was corrupted by 20 dB SNR. Assuming that there is no prior knowledge about the frequency of the inter-area mode, the data window length was set as 10 s as explained in Section 2.4. The event detection logic identified an onset of a ring-down oscillation at time, $t = 5.33$ s. Table 8 shows the average values of the mode parameters over two data windows selected just after and few seconds later the application of the disturbance.

Table 8 also highlights that the damping estimation deviates from the value obtained from the eigenvalue analysis when a data window soon after the disturbance is processed. Further, among these two data windows, the improved Prony algorithm extracted another

mode at 1.149 Hz and 5.4% in the first data window. The eigenvalue analysis also showed an oscillatory mode at 1.142 Hz and damping ratio of 5.32%. It can be also seen from Fig. 8 that a single mode is dominating over the second data window 20.6–30.6 s. Furthermore, among the 100 independent trials, the algorithm extracted only the true mode in 99 trials in the first data window and 92 trials in the second data window.

5.3 Discussion

In this study, the performance of the proposed oscillation monitoring algorithm was investigated using a PC having an Intel Core i7 processor (3.40 GHz) with 8 GB RAM. The computational burden of the algorithm was acceptable for updating the mode extraction results at an interval of around half a second. Furthermore, it is recommended to store the frequencies and the damping ratios of the true modes calculated over a predetermined number of data windows, say 3 and check the consistency of the parameters before indicating to the operator. This consistency check would further improve the accuracy of the conclusion. The actual PMU measurements can also have missing data points as well as abnormal data points. The problem of missing data points can be eliminated by replacing them using interpolation as proposed in [13, 14]. The presence of an abnormal data point is indicated by a sudden spike in the ratio

$$\frac{|y(k) - y(k-1)|}{\Delta t},$$

where Δt is the sampling time. Now, replacement of the abnormal data point $y(k)$ by $y(k-1)$ enhances the performance of the algorithm.

The main goal of this paper was to show that the proposed improved Prony algorithm can be used for real-time monitoring of the low-frequency oscillations. The conventional Prony algorithm can also be applied on multiple measurements of the power system to identify these oscillations. The application of the multisignal Prony analysis in this regard has been investigated in [9, 17].

Fig. 8 *Active power output of generator 16 subsequent to a contingency*

However, this approach needs more offline analysis to identify which multiple measurements to be used to determine the mode parameters. For example, a series of empirical rules have been developed in [9] for selecting the power system variables to monitor the low-frequency oscillations. In contrast, the improved Prony algorithm presented in this paper can be applied individually to multiple signals measured at different locations. This is useful when all the interested modes are not observable at a single location. Furthermore, the improved Prony algorithm presented in this paper can also be used in other applications, such as (i) studying outputs of transient stability programs [6], and (ii) offline analysis of field measured data [18].

6 Conclusions

It has been shown that the dominant low-frequency modes in ring-down oscillations in power systems can be extracted using Prony models with varying orders. In order to change the order of the Prony model, a shrinking window approach and a multiple sampling time approach have been proposed. This paper presented an oscillation monitoring algorithm, including the improved Prony algorithm to monitor the inter-area oscillations in real time. It has been shown that the true mode parameters determined by the algorithm are less sensitive to the amount of noise present in the input signal and to the different PMU reporting rates recommended by the IEEE standard for synchrophasor measurements in power systems. The simplicity, true mode extraction capability, accurate determination of the mode parameters, and the acceptable computing time are the indicators of the applicability of the proposed algorithm for wide-area monitoring of power system oscillations.

7 References

1 Kelin, M., Rogers, G.J., Kundur, P.: 'A fundamental study of inter-area oscillations in power systems', *IEEE Trans. Power Syst.*, 1991, **6**, (2), pp. 914–921
2 Pouyan, P., Kundur, P.S., Taylor, C.W.: 'The anatomy of a power grid blackout-root causes and dynamics of recent major blackouts', *IEEE Power Energy Mag.*, 2006, **4**, (5), pp. 22–29
3 Kosterev, D.N., Taylor, C.W., Mittelstadt, W.A.: 'Model validation for the August 10, 1996 WSCC system outage', *IEEE Trans. Power Syst.*, 1999, **14**, (3), pp. 967–979
4 IEEE Std. C37.118.1: 'IEEE standard for synchrophasor measurements for power systems', 2011
5 Thambirajah, J., Barocio, E., Thornhill, N.F.: 'Comparative review of methods for stability monitoring in electrical power systems and vibrating structures', *IET Gener. Transm. Distrib.*, 2010, **4**, (10), pp. 1086–1103
6 Hauer, J.F., Demeure, C.J., Scharf, L.L.: 'Initial results in Prony analysis of power system response signals', *IEEE Trans. Power Syst.*, 1990, **5**, (1), pp. 80–89
7 Korba, P., Larsson, M., Rehtanz, C.: 'Detection of oscillations in power systems using Kalman filtering techniques'. Proc. IEEE Conf. Control Applications, June 2003, pp. 186–188
8 Gasca, J.J.S., Chow, J.H.: 'Computation of power system low-order models from time domain simulations using a Hankel matrix', *IEEE Trans. Power Syst.*, 1997, **12**, (4), pp. 1461–1467
9 Quintero, J., Guoping, L., Venkatasubramaniam, V.M.: 'An oscillation monitoring system for real-time detection of small-signal instability in large electric power systems'. Proc. IEEE Power and Energy Society General Meeting, June 2007, pp. 1–8
10 Gasca, J.J.S., Chow, J.H.: 'Performance comparison of three identification methods for the analysis of electromechanical oscillations', *IEEE Trans. Power Syst.*, 1999, **14**, (3), pp. 995–1002
11 Messina, A.R., Vittal, V., Vega, D.R., Harper, G.E.: 'Interpretation and visualization of wide-area PMU measurements using Hilbert analysis', *IEEE Trans. Power Syst.*, 2012, **21**, (4), pp. 1763–1771
12 Kamwa, I., Pradhan, A.K., Joos, G.: 'Robust detection and analysis of power system oscillations using the Teager-Kaiser energy operator', *IEEE Trans. Power Syst.*, 2011, **26**, (1), pp. 323–333
13 Tashman, Z., Khalilinia, H., Venkatasubramanian, V.: 'Multi-dimensional Fourier ringdown analysis for power systems using synchrophasors', *IEEE Trans. Power Syst.*, 2014, **29**, (2), pp. 731–741
14 Zhou, N., Pierre, J.W., Trudnowski, D.J., Guttromson, R.T.: 'Robust RLS method for online estimation of power system electromechanical modes', *IEEE Trans. Power Syst.*, 2007, **22**, (3), pp. 1240–1249
15 Power Tec. Lab, BC, Canada: 'Transient Security Assessment Tool (TSAT) User manual', 2009
16 Zhou, N., Pierre, J.W., Trudnowski, D.: 'A stepwise regression method for estimating dominant electromechanical modes', *IEEE Trans. Power Syst.*, 2012, **27**, (2), pp. 451–458
17 Trudnowski, D.J., Johnson, J.M., Hauer, J.F.: 'Making Prony analysis more accurate using multiple signals', *IEEE Trans. Power Syst.*, 1999, **14**, (1), pp. 226–231
18 Trudnowski, D.J.: 'Order reduction of large-scale linear oscillatory system models', *IEEE Trans. Power Syst.*, 1994, **9**, (1), pp. 451–458
19 Kumaresan, R., Tufts, D.W.: 'Estimating the parameters of exponentially damped sinusoids and pole-zero modeling in noise', *IEEE Trans. Acoust., Speech Signal Process.*, 1982, **ASSP-30**, (6), pp. 833–840
20 Lin, C.M., Vittal, V., Kliemann, W., Fouad, A.A.: 'Investigation of modal interaction and its effects on control performance in stressed power systems using normal forms of vector fields', *IEEE Trans. Power Syst.*, 1996, **11**, (2), pp. 781–787
21 Sanchez_Gasca, J.J., Vittal, V., Gibbard, M.J., *et al.*: 'Inclusion of higher order terms for small-signal (modal) analysis: committee report-task force on assessing the need to include higher order terms for small-signal (modal) analysis', *IEEE Trans. Power Syst.*, 2005, **20**, (4), pp. 1886–1904
22 Vien, A.: 'Practical numerical issues in industrial identification'. PhD dissertation, Univ. of Alberta, 1994
23 Zhou, N., Huang, Z., Tuffner, F., Pierre, J., Jin, S.: 'Automatic implementation of Prony analysis for electromechanical mode identification from phasor measurements'. Proc. IEEE Power and Energy Society General Meeting, July 2010, pp. 1–8
24 Proakis, J.G., Manolakisl, D.G.: 'Digital signal processing: principles, algorithms and applications' (Prentice-Hall, 2007, 4th edn.)
25 Peng, J.C.-H., Nair, N.-K.C.: 'Adaptive sampling scheme for monitoring oscillations using Prony analysis', *IET Gener. Transm. Distrib.*, 2009, **3**, (12), pp. 1052–1060
26 Chaudhuri, B., Pal, B.: 'Robust control in power systems' (Springer, 2005)
27 Jayasekara, K.Y.B.D.S.: 'Determination of transient stability boundary in functional form with applications in optimal power flow and security control'. PhD dissertation, University of Manitoba, 2006